PFC/JA–89–45

Growth and Frequency Pushing Effects in Magnetron Phase–Locking

Chen, S.C.

Plasma Fusion Center
Massachusetts Institute of Technology
Cambridge, MA 02139

October 1989

This work was supported by Harry Diamond Labs (Army) Contract DAAL02–89–K–0084

Growth and Frequency Pushing Effects in Magnetron Phase-Locking

S.C. Chen

Plasma Fusion Center

Massachusetts Institute of Technology, Cambridge, MA 02139

ABSTRACT

A magnetron-specific equivalent-circuit model has been developed which takes into account the unconventional magnetron growth characteristics as well as the frequency pushing effect. These effects, which owe their origin to the highly nonlinear electron-wave interaction, are shown to play important roles in the magnetron phase locking process. The model predicts a wider locking-bandwidth and a shorter locking time than those in conventional locking theory. The phase-locked amplitude resonance occurs, as the results indicated, at an injection frequency different from that of the free-running oscillator.

I Introduction

The past ten years have seen the rapid progress made in the research on high power microwaves.[1-3] Phase control of high power oscillators appears to be the logical and the promising means for harnessing and enhancing the unprecedented power output.[4-6] The relativistic magnetron, with its reentrant nature and high efficiency, is an especially desirable candidate as the heart of a phase-locked system.[7-9] Research in this area has been very active and major results were achieved recently in a short-pulse experiment.[10] Long-pulse operation[11-14] and the subsequent phase-locking[15] of relativistic magnetrons, provide more interesting application possibilities and involve greater technical challenges not encountered in the short-pulse experiments.

Frequency pushing effect, which has been observed experimentally in relativistic magnetrons recently,[16] was identified and proved to be of critical importance in obtaining phase control.[17,18] On the other hand, phase locking of pulsed oscillators — especially those with a cavity fill time comparable with (or not much longer than) the pulse length — requires attention to the details of the magnetron growth process. The ubiquitous van der Pol equation[19] lacks both the magnetron-specific growth and frequency pushing effects; hence will not serve the purpose of a magnetron model equation. However, the highly nonlinear crossed-field interaction in magnetrons involves very complex geometry and particle dynamics, hence the grow-frequency characteristics (or, equivalently, the dispersion relation) cannot be calculated easily from first principles. It is the purpose of this paper to temporarily de-emphasize the differences between the relativistic and the conventional magnetrons, and to apply the conceptually simple approach — modelling the growth/frequency features within the lumped-circuit model — to obtain fundamental understanding of the phase-locking behavior in magnetrons.

Section II discusses the operating features of magnetrons and justifies the choice of model equations for the electronic conductance and susceptance using two independent simulation techniques. An equivalent circuit model based on the model equations is constructed, followed by an analysis of the free-running oscillator state. In section III, phase

locking with weak injection near the oscillator frequency is analyzed. Important effects due to the magnetron–specific features are identified.

II. Signal growth and frequency-pushing in magnetrons

One distinct feature that sets magnetrons apart from other oscillators is the growth and saturation characteristics. This is illustrated qualitatively in Figure 1, in which the electronic conductance g (the ratio of RF current and RF voltage) is plotted against the RF voltage. The conductance curve for magnetrons (Figure 1a) assumes a "concave" shape with a second derivative greater than zero. This phenomenon, namely the existence of finite RF current even with very small RF voltage, has long been observed in magnetron operation.[20,21] The state of zero current is extremely unstable which, with very small perturbation, breaks into a state of large current. This behavior, which differs drastically from that of most conventional self-excited oscillators (Figure 1b), leads to some unique properties in magnetrons to be described in the following.

To model this magnetron feature, Slater[20,21] suggested using

$$g = \frac{1}{R}\left(\frac{V_{DC}}{V_{\mathrm{RF}}} - 1\right) \tag{1}$$

to relate the conductance to the rms RF-voltage (see Figure 1a). This is to be compared with the more conventional expression for other oscillators (Figure 1b)

$$g = g_0\left(1 - \frac{{V_{\mathrm{RF}}}^2}{{V_{DC}}^2}\right) \tag{2}$$

(where g_0 is the small-signal gain) which can often be derived from first principles.[19]

In addition to the in-phase component of the RF current which governs the temporal growth, of equal importance is the contribution from the out-of-phase RF current which determines the output frequency. Frequency-pushing, namely the frequency change caused by the presence of the electron space charge — the same space charge responsible for the gain —, is modeled by the following expression[20,21]

$$b = b_0 - g \cdot tan\alpha. \tag{3}.$$

The relationship between the real and imaginary parts of the frequency (susceptance b and conductance g) is evident from Figure 1. It should not be surprising that the frequency

pushing effect, represented by the pushing parameter α of order unity, plays a major role in magnetron phase locking since the angle α characterizes the phase lag between the electron bunch and the resonant wave. In simple devices like reflex klystrons, the angle α is found to be the deviation of the average transit-time from $\frac{2}{3}\pi$ (for $1\frac{3}{4}$-mode) in the repeller region.[21] It is believed the angle α in magnetrons is directly related to the angle between the rotating electron spoke and the RF voltage peak.

To justify the choice of the model equation (1), we have[22] extended an existing semi-empirical model of conventional magnetrons[23–27] and applied the model to examine the behavior of the electronic conductance. The important variable in this theory is α, the relative phase angle between the rotating space charge spoke and the RF-peak. By assuming the existence of spokes with shapes suggested by particle simulations[28,29], and with a charge density distribution given by the Brillouin model[30], the electron currents are calculated under synchronism conditions. Each spoke is treated as one macroparticle with assigned charge and calculated average velocity components. The RF field in the cavity is calculated from the energy conservation equation, which involves modeling the particle loss mechanisms in the anode and cathode as well as the RF loss due to the finite cavity Q. With the system of equations, it is possible to find the operating point self-consistently, and to predict the saturated power level and the output frequency. Such a model scales correctly over a wide range of known magnetron designs.[23]

We have developed a computer program based on this model and applied it to the 4J50 magnetron (high power X-band, see Vaughan[23] for tube parameters). By changing the loading level at the output, the corresponding operating RF-amplitudes under steady-state condition were monitored. The result is shown in Figure 2a. We have[22] successfully reproduced the gain characteristics (Figure 2a) described by Eq.(1).

A second approach was taken by Dombrowsky[31] using a more elaborate simulation scheme.[32] The result of the simulation is shown in Figure 2b.

The spoke model[22] and the Dombrowski simulation[31] thus provide independent means of confirming the $1/V_{\mathrm{RF}}$ dependence of the magnetron growth.

Based on the magnetron-specific models for g and b described in equations (1) and (3), we then proceed to construct an equivalent-circuit model and study the steady-state and the phase-locking operation in magnetrons.

The model is based upon the general oscillator equation derived from the standard parallel RLC circuit (see Figure 3). The magnetron gain mechanism is represented by a shunt electronic admittance $g + ib$. The single-mode oscillator equation for this circuit is

$$\frac{g+ib}{C\omega_0} = i(\frac{\omega}{\omega_0} - \frac{\omega_0}{\omega}) + \frac{1}{Q_0} + \frac{G+iB}{Q_{ext}}, \tag{4}$$

where $G + iB$ is the voltage-dependant nonlinear complex admittance of the load. In the equation, ω is the output frequency, $\omega_0 = \frac{1}{\sqrt{LC}}$, $Q_0 = RC\omega_0$, and Q_{ext} is the external Q.

Inserting (1) and (3) into (4), and separating the real and imaginary parts, the steady-state values of the amplitude V_{RF0} and frequency ω' for a free running magnetron are found to be

$$V_{RF0} = \frac{V_{DC}}{2RC} \frac{1}{\frac{1}{2}\omega_0(\frac{1}{Q_L} + \frac{1}{RC\omega_0})} \tag{5},$$

and

$$\omega' = \omega_0 + \frac{1}{2}(\frac{b_0}{C} - \frac{B\omega_0}{Q_{ext}}) - \frac{\omega_0 \cdot tan\alpha}{2Q_L}. \tag{6}$$

Equation (6) contains both the frequency pulling ($\frac{B\omega_0}{Q_{ext}}$) as well as the pushing $\frac{\omega_0 \cdot tan\alpha}{2Q_L}$ terms. We define a growth parameter

$$\gamma = \frac{1}{2}\omega_0(\frac{1}{Q_L} + \frac{1}{RC\omega_0}) \tag{7}$$

for later convenience. The amplitude and frequency evolution in magnetron start-up phase can be calculated under situations when the frequency is much greater than the growth rate $\omega \gg \gamma$, hence the growth process can be approximated adiabatically by a succession of instantaneous steady-state solutions. The oscillator equation is then modified by the addition of a temporal growth rate $-i\Gamma(t)$ to the frequency ω

$$\frac{g+ib}{C\omega_0} = i(\frac{\omega - i\Gamma}{\omega_0} - \frac{\omega_0}{\omega - i\Gamma}) + \frac{1}{Q_0} + \frac{G+iB}{Q_{ext}}, \tag{8}$$

where

$$\Gamma(t) = \frac{\dot{V}_{RF}}{V_{\mathrm{RF}}}. \tag{9}$$

The real part of (8) again governs the growth

$$\frac{g}{C\omega_0} = \frac{1}{Q_L} + \frac{2}{\omega_0}\Gamma(t). \tag{10}$$

Inserting (1) into (10) and using the definition of Γ (Eq. (9)), one obtains the RF amplitude equation

$$\dot{V}_{RF} = -\gamma \cdot (1 - \frac{V_{RF0}}{V_{\rm RF}}) \cdot V_{\rm RF}. \tag{11}$$

The solution of (10) gives the RF amplitude evolution in magnetrons

$$V_{\rm RF}(t) = V_{RF0} \cdot (1 - \eta e^{-\gamma t}), \tag{12}$$

where

$$\eta = 1 - \frac{V_i}{V_{RF0}} \sim 1 \tag{13}$$

characterizes the initial signal level in the tube. The interesting implication is that the stage of starting from noise is rapidly passed through, and a linear (not exponential) build-up then brings the system to saturation in a manner similar to a capacitor charging up. The detail mechanism behind these observations for magnetrons, however, remains largely unexplored.

Solving the equation obtained by taking the imaginary part of (8), one finds that the output frequency evolves according to

$$\omega(t) = \omega' - tan\alpha \cdot \gamma \cdot \frac{\eta e^{-\gamma t}}{1 - \eta e^{-\gamma t}}, \tag{14}$$

and approaches the steady-state free running frequency ω' defined in Eq.(6).

III. Phase locking of magnetrons

We follow the techniques developed in previous work[20,21,33,34] and treat the locking source as part of the magnetron load which injects counter propagating I_1 and V_1 at a frequency ω_1. The total admittance, including the locking source, at the load for the driven magnetron is

$$\begin{aligned} Y(t) &= \frac{Ie^{i\omega t} + I_1 e^{i\omega_1 t}}{Ve^{i\omega t} + V_1 e^{i\omega_1 t}} = \frac{I}{V} \cdot \frac{1 + \frac{I_1}{I} e^{i(\omega_1 - \omega)t}}{1 + \frac{V_1}{V} e^{i(\omega_1 - \omega)t}} \\ &= \frac{I}{V} \cdot [1 + (\epsilon_I - \epsilon_V) e^{i(\omega_1 - \omega)t} + (\epsilon_V^2 - \epsilon_V \epsilon_I) e^{2i(\omega_1 - \omega)t} + O(\epsilon_V^3)], \end{aligned} \tag{15}$$

where

$$\epsilon_V = \frac{V_1}{V}, \qquad \epsilon_I = \frac{I_1}{I}. \tag{16}$$

Consider the case of injection locking with a weak reference signal and neglect the $O(\epsilon_V^2)$ terms in (15), the admittance simplifies to

$$Y(t) \sim (G + iB) \cdot (1 + (\epsilon_I - \epsilon_V) e^{i(\omega_1 - \omega)t}), \tag{17}$$

where $G + iB$ is the matched load admittance as in Figure 3. It is convenient to define the injection parameter ρ , the injection phase θ_i, and the relative phase θ as follows:

$$\rho = \frac{1}{2}(\epsilon_I - \epsilon_V) \cdot \sqrt{G^2 + B^2} \tag{18}$$

$$\theta_i = sin^{-1} \frac{B}{\sqrt{G^2 + B^2}} \tag{19}$$

$$\theta(t) = \phi_{Mag}(t) - (\omega_1 t + \theta_i). \tag{20}$$

Introducing the total load admittance (17) into the oscillator equation (4)

$$\frac{g + ib}{c\omega_0} = i(\frac{\omega}{\omega_0} - \frac{\omega_0}{\omega}) + \frac{1}{Q_0} + \frac{G + iB + 2\rho e^{-i[\phi - (\omega_1 t + \theta_i)]}}{Q_{ext}}, \tag{21}$$

and separating the real and imaginary parts, we have

$$\frac{g}{c\omega_0} = \frac{1}{Q_L} + \frac{2\rho cos\theta}{Q_{ext}} \tag{22}$$

$$\frac{b}{c\omega_0} = \frac{2(\omega - \omega_0)}{\omega_0} + \frac{B}{Q_{ext}} - \frac{2\rho sin\theta}{Q_{ext}}. \tag{23}$$

In deriving (23), we have assumed $\omega \sim \omega_0$ for simplicity. This formulation is valid for oscillators in general, since the form of g and b has not been specified yet.

It is interesting to point out that although the magnetron-specific features (1) and (3) were repetitively described and emphasized in Slater's work[20,21], they were not included in his phase locking calculations.[20] Here we introduce Eqs. (1) and (3) into Eqs. (22) and (23) , and obtain the equations for driven magnetrons. The equations governing the amplitude and the frequency evolution are

$$V_{\rm RF}(t) = V_{RF0}\frac{1}{1+\frac{\rho\omega_0 cos\theta(t)}{Q_{ext}\gamma}} \tag{24}$$

and

$$\omega(t) - \omega' = \frac{\rho\omega_0}{Q_{ext}}(sin\theta(t) - cos\theta(t)\cdot tan\alpha). \tag{25}$$

To simplify the equations, we normalize all frequencies with respect to ω_0 and introduce the dimensionless injection and detuning parameters into (24) and (25)

$$\mu = \frac{\rho}{Q_{ext}}, \quad \sigma = \frac{\omega' - \omega_1}{\omega_0}. \tag{26}$$

The resultant equations

$$V_{\rm RF}(t) = V_{\rm RF}(\theta(t)) = V_{RF0}\frac{1}{(1+\frac{\mu}{\gamma}\cos\theta(t))}, \tag{27}$$

and

$$\frac{d\theta}{dt} = \frac{\mu}{\mid cos\alpha \mid}sin(\theta-\alpha) + \sigma \tag{28}$$

describe the amplitude and the relative phase evolution. It is important to realize the parameter range in which the analysis is valid. The assumptions we have made so far can be conveniently collected in terms of a simple inequality which relates frequency, growth parameter, injection amplitude, pushing parameter, and frequency difference:

$$1 = \omega_0 > \gamma \geq \frac{\mu}{\mid cos\alpha \mid} \geq \mid \sigma \mid . \tag{29}$$

The condition under which phase locking occurs is obtained by setting (28) to zero for steady-state,

$$\frac{\mu}{\mid cos\alpha \mid} \geq \sigma, \tag{30}$$

which reduces to the familiar Adler's condition[35] $\mu \geq \sigma$ when the frequency pushing parameter α is zero. The widening of the locking frequency range can be quite appreciable depending on the amount of frequency pushing. The experimentally observed magnitude of α ranges roughly from 0 to 1.5 depending on the operating DC voltage. Under normal operating condition, it is on the low side. An α of 0.25 is chosen as the typical value and is used in the following analysis. The final relative phase of the locked system is also modified by the nonzero pushing parameter α

$$\theta_{lock} = sin^{-1}(-\frac{\sigma \mid cos\alpha \mid}{\mu}) + \alpha. \tag{31}$$

To summarize the steady-state behavior of the weak injection phase locking system near the fundamental locking zone, we combine the phase and amplitude equations (27) and (28) by cancelling the θ–dependance. The resultant equation

$$\frac{(\frac{V_{RF}}{V_{RF0}} - 1)^2}{(\frac{\mu}{\gamma})^2} = (\pm\sqrt{1 - (\frac{\sigma}{\mu'})^2}\ cos\alpha + \frac{\sigma}{\mu'} sin\alpha)^2 \tag{32}$$

contains the dependance of output amplitude V_{RF} on three parameters: the injection parameter $\mu' = \mu/\mid cos\alpha \mid$, the pushing parameter α, and the detuning parameter σ. The effect of the frequency pushing can be singled out by comparing the above equation with the case when $\alpha = 0$

$$\frac{(\frac{V_{RF}}{V_{RF0}} - 1)^2}{(\frac{\mu}{\gamma})^2} + \frac{\sigma^2}{\mu^2} = 1\ , \qquad \alpha = 0. \tag{33}$$

Figure 4 illustrates this comparison by showing the loci of the steady phase-locked states on the σ–V_{RF} plane for $\gamma = .1$. Different curves correspond to different values of injection amplitudes μ. Figure 4 depicts the dependance of V_{RF} on σ for the case of (a) no frequency pushing ($\alpha = 0$), and (b) finite frequency pushing ($\alpha = 0.25$). The free-running state is represented by the point $\sigma = 0, V_{RF}/V_{RF0} = 1$. It is clearly seen in Figure 4a, that the loci of the phase locked states for weak injection form a family of "ellipses" with an eccentricity $\epsilon = \sqrt{1 - \gamma^2}$. The deviation of the "ellipses" from exact elliptical shape is caused by the unconventional form of the growth model (1); the results obtained for conventional oscillators based on (2) form evenly spaced ellipses with a common geometric

center. Characterized by an injection parameter μ, each ellipse in Figure 4 consists of two branches. The result of a stability analysis established the existence of a stability criteria ($\cos\theta_{lock} \leq 0$), shown in Figure 4 as the dashed line. Only the upper branch of the double-valued ellipses constitutes the stable solutions.

A nonzero α causes the ellipses to rotate around the origin (Figure 4b) . In phase-locked states, the frequency pushing effectively rotates the ellipses by an angle

$$\theta_1 = tan^{-1}(\gamma\ sin\alpha), \tag{34}$$

which results in a wider locking bandwidth, as described by (30), than the conventional Adler's condition. The maximum power output, that is, the amplitude resonance, occurs at an injection frequency detuned from the free-running value

$$\sigma_m = \mu\ sin\alpha. \tag{35}$$

The amount of detuning, namely the difference of the optimal injection frequency and the free-running frequency, can become appreciable with large μ. For example, the detuning can be 1% for a μ of 0.4.

The boundary between the stable and the unstable branches, shown in Figure 4 as the dashed line, is also tilted by an angle

$$\theta_2 = tan^{-1}\frac{sin2\alpha}{2\gamma(1-(\frac{\mu sin\alpha}{\gamma})^2)} \sim tan^{-1}\frac{sin2\alpha}{2\gamma}. \tag{36}$$

The tilting effectively makes the phase-locked power output asymmetrical with respect to the injection frequency.

Transient behavior is of special interests in the case of phase locking pulsed oscillators. The transient solution for the locking process is obtained by integrating (28) with respect to time. For the locking case ($\sigma < \mu'$), the relative phase evolves according to

$$\theta(t) = 2\ tan^{-1}(-\frac{\mu'}{\sigma} + \frac{A}{\sigma}\frac{1+De^{At}}{1-De^{At}}) + \alpha, \tag{37}$$

where

$$A = \sqrt{\mu'^2 - \sigma^2} \tag{38}$$

is the characteristic time and

$$D = \frac{\sigma \ tan\frac{-\theta_i - \alpha}{2} + \mu' - A}{\sigma \ tan\frac{-\theta_i - \alpha}{2} + \mu' + A} \tag{39}$$

is the parameter characterizing the amplitude of the transient. It is easily shown that $\theta(0) = -\theta_i$, and $\theta(\infty) = \theta_{lock}$. As (37) indicates, phase locking is a continuous process which occurs on a time scale T_{lock}. The locking time T_{lock} is a function of (A,D), which in turn depends on the parameter set $(\mu, \sigma, \alpha, \theta_i)$. Using (37)–(39), it can be proved, and has been demonstrated by numerical examples, that the frequency pushing effect ($\alpha \neq 0$) shortens the locking time independent of the sign of α!

For the unlocked case ($\sigma > \mu'$), the relative phase evolves according to

$$\theta(t) = 2 \ tan^{-1}\left(\frac{A'q + (\mu'q + \sigma) \cdot tan\frac{A'}{2}t}{A'q - (\sigma q + \mu') \cdot tan\frac{A'}{2}t}\right) + \alpha, \tag{40}$$

where

$$A' = \sqrt{\sigma^2 - \mu'^2}, \tag{41}$$

and

$$q = tan\frac{-\theta_i - \alpha}{2}. \tag{42}$$

In the extreme case when the two frequencies are far apart ($\mu' \ll \sigma$), simple beating is recovered

$$\theta(t) = -\theta_i + \sigma \cdot t. \tag{43}$$

IV. Conclusion

We have constructed a magnetron-specific equivalent-circuit model for the study of the steady-state and the phase-locking operation in magnetron oscillators. The unconventional magnetron growth characteristics lead us to believe that the state of pre-oscillation equilibrium is extremely unstable which, with very small perturbation, breaks into a state of large current. The magnetron growth process rapidly passes through the stage of starting up from noise, followed by a linear (not exponential) build-up which then brings the system to saturation. More theoretical effort is needed to explain the phenomena.

Besides the growth characteristics, the frequency pushing manifests itself in many important effects in magnetron phase locking. Among which: the locking bandwidth is wider than the usual Adler condition; the resonance of the phase-locked amplitude occurs at frequencies different from the free-running frequency; the time required for locking to occur is shortened by the frequency pushing effect; and the relative phase of the locked-state is modified by the pushing parameter.

Recently, the importance of frequency pushing effect on the phase locking of regenerative oscillators has also been identified and studied by modeling the nonlinear frequency shift with a Duffing (cubic restoring force) term in a van der Pol oscillator.[17,18] The connection between the two frequency pushing effect models — namely the van der Pol/Duffing oscillator and the magnetron equivalent circuit model — is currently under study. It is also possible to construct a magnetron oscillator differential equation containing both the growth and the frequency features, which will be applied to the modelling of general magnetron related phenomena on the oscillation time scale.

Acknowledgement

I am grateful to G. Bekefi, R.C. Davidson, G.L. Johnston, and R. Temkin for very useful discussions. This work was supported by SDIO/IST, and managed by Harry Diamond Laboratories.

REFERENCE

[1]V.L. Granatstein and I.A. Alexeff, Editors, *High Power Microwave Sources*, Artech House (1987).

[2]N. Rostoker, Editor, *Microwave and Particle Beam Sources and Propagation*, Proc. SPIE 873 (1988).

[3]H.E. Brandt, Editor, *Microwave and Particle Beam Sources and Directed Energy Concepts*, Proc. SPIE 1061 (1989).

[4]D. Price, H. Sze, and D. Fittinghoff, *J. Appl. Phys.*,**65**, 5185 (1989).

[5]A.W. Fliflet and W.M. Manheimer,*Phys. Rev. A*, **39**, 3432 (1989).

[6]W. Woo, J. Benford, D., Fittinghoff, B. Harteneck, D. Price, R. Smith, and H. Sze, *J. Appl. Phys.*,**65**, 861 (1989).

[7]W.C. Brown,*IEEE Trans. MTT*, **MTT-21**, 753 (1973).

[8]P.B. Wilson, SLAC Pub. 4803, Dec. (1988).

[9]T. Overett, D.B. Remsen, E. Bowles, G.E. Thomas, and R.E. Smith, III, IEEE Particle Accelerator Conf., 1464 (1987).

[10]J. Benford, H.M. Sze, W. Woo, R.R. Smith, and B. Harteneck , *Phys. Rev Lett.*, **62**, 969 (1989).

[11]S.C. Chen and G. Bekefi, "Relativistic Magnetron Research", N. Rostoker, Editor, Proc. SPIE **873**, 18 (1988).

[12]A.G.Nokonov, I.M. Roife, Yu.M. Savel'ev, and V.I. Engel'ko, *Sov. Tech. Phys.*, **32**, 50 (1987).

[13]A.N. Didenko, A.S. Sulakshin, G.P. Fomenko, V.I. Tsvetkov, Yu. G. Shtein, and Yu.G.Yushkov, *Sov. Tech. Phys. Lett.*, **4**, 331 (1979).

[14]I.Z. Gleizer, A.N. Didenko, A.S. Sulakshin, G.P. Fomenko, and V.I. Tsvetkov, *Sov. Tech. Phys. Lett.*, **6**, 19 (1980).

[15]S.C. Chen, G. Bekefi, R. Temkin, and C. de Graff, "Proposed Injection Locking of a Long Pulse Relativistic Magnetron", H.E. Brandt, Editor, Proc. SPIE **1061**, 157 (1989).

[16]I.I. Vintizenko, A.S. Sulakshin, and G.P. Fomenko, *Sov. Tech. Phys. Lett.*, **13**, 579 (1987).

[17]J.E. Walsh, G.L. Johnston, R.C. Davidson, and D.J. Sullivan, SPIE Proceedings **1061**, 161 (1989).

[18]H. Lashinsky, Periodic Nonlinear Phenomena, unpublished manuscript.

[19]B. van der Pol, *Phil. Mag.* S. 7. Vol. 3, No.13 (1927).

[20]J.C. Slater, R.L.E. Technical Report No. 35, M I T (1947).

[21]J.C. Slater, *Microwave Electronics* (1954).

[22]S.C. Chen, G. Bekefi, and D.P. Aalberts, to be published.

[23]J. R. M. Vaughan, IEEE Trans. Electron Devices, **ED-20**, 818 (1973); J. R. M. Vaughan, IEEE Trans. Electron Devices, **ED-21**, 132 (1974).

[24]A. Azumi, *Fujitsu Sci. Tech. J.*, vol. 7, no. 1 (1971).

[25]J. F. Hull, *IRE Trans. Electron Devices*, **ED-8** (1961).

[26]J. F. Hull, Ph.D. dissertation, Polytechnic Institute of Brooklyn (1958).

[27]H. W. Welch, *Proc. IRE*, **41**, 11 (1953).

[28]A. Palevsky and G. Bekefi, *J. Appl. Phys.*, **52**, 4938 (1981).

[29]L.D. Ludeking, G.E. Thomas, W.M. Bollen, IEDM , 160 (1987).

[30]J. Swegle and E. Ott, *Phys. Fluids* **24**, 10 (1981).

[31]G.E. Dombrowski, private communication.

[32]G.E. Dombrowski, IEEE Trans. Electron Devices, **ED-35**, 2060 (1988).

[33]E.E. David, R.L.E. Technical Report No. 100, M I T (1949).

[34]E.E. David, in *Crossed Field Microwave Devices*, vol.2, E. Okress Ed., 375 (1961).

[35]R. Adler, Proc. IRE vol.34, 351 (1946).

Figure Captions

Figure 1 Electronic conductance g and susceptance b as functions of the rms voltage in the RF-field for (a) magnetrons, and (b) conventional regenerative oscillators.

Figure 2 Calculated magnetron electronic conductance g as a function of V_{RF}. (a) The 4J50 magnetron operating at steady-state with three different DC-voltages are calculated using macro-spoke model (Chen). (b) The 2J32 magnetron starting up from injected noise is calculated using macro-particle simulation (Dombrowski). Both (a) and (b) produced the g–dependance described by the model equation (1).

Figure 3 Equivalent circuit used in modelling magnetron operation. $g+ib$ is the complex admittance describing the electron-wave interaction. $G+iB$ represents the load admittance. RLC-circuit models the magnetron resonance cavity with loss.

Figure 4 Amplitude $(\frac{V_{\mathrm{RF}}}{V_{\mathrm{RF}0}})$ versus normalized frequency difference σ in the phase-locked states for three injection amplitudes $\mu = 0.01, 0.02, 0.03$. (a) No frequency pushing, each ellipse corresponds to an injection parameter μ. (b) The effect of frequency pushing ($\alpha = 0.25$) rotates the ellipses and results in a wider locking bandwidth and a shifted amplitude resonance frequency.

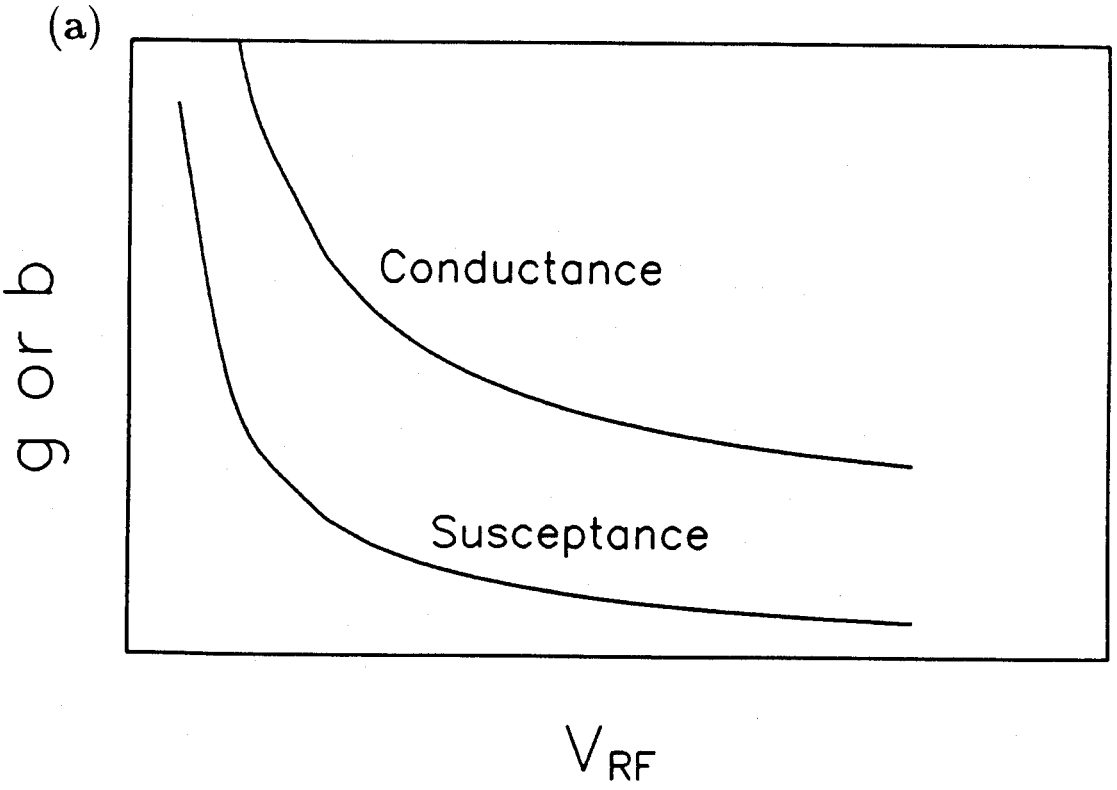

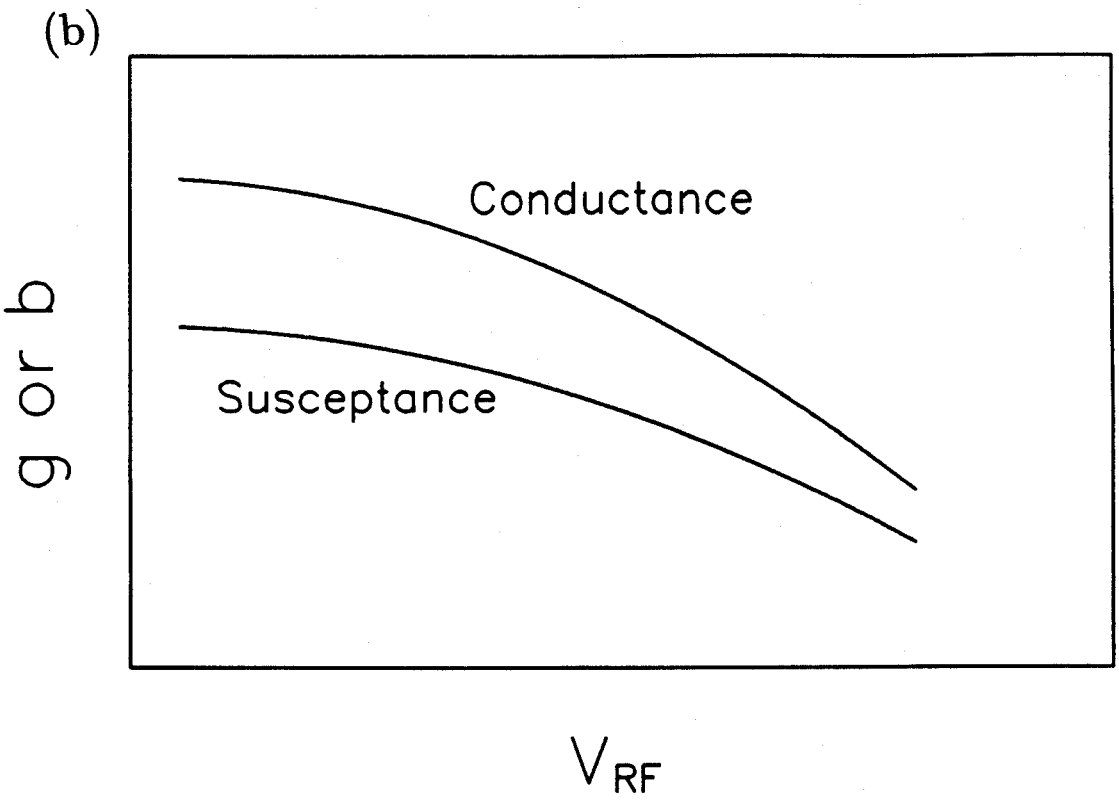

Figure 1 Electronic conductance g and susceptance b as functions of the rms voltage in the RF-field for (a) magnetrons, and (b) conventional regenerative oscillators.

(a)

Figure 2 Calculated magnetron electronic conductance g as a function of V_{RF}. (a) The 4J50 magnetron operating at steady-state with three different DC-voltages are calculated using macro-spoke model (Chen). (b) The 2J32 magnetron starting up from injected noise is calculated using macro-particle simulation (Dombrowski). Both (a) and (b) produced the g-dependance described by the model equation (1).

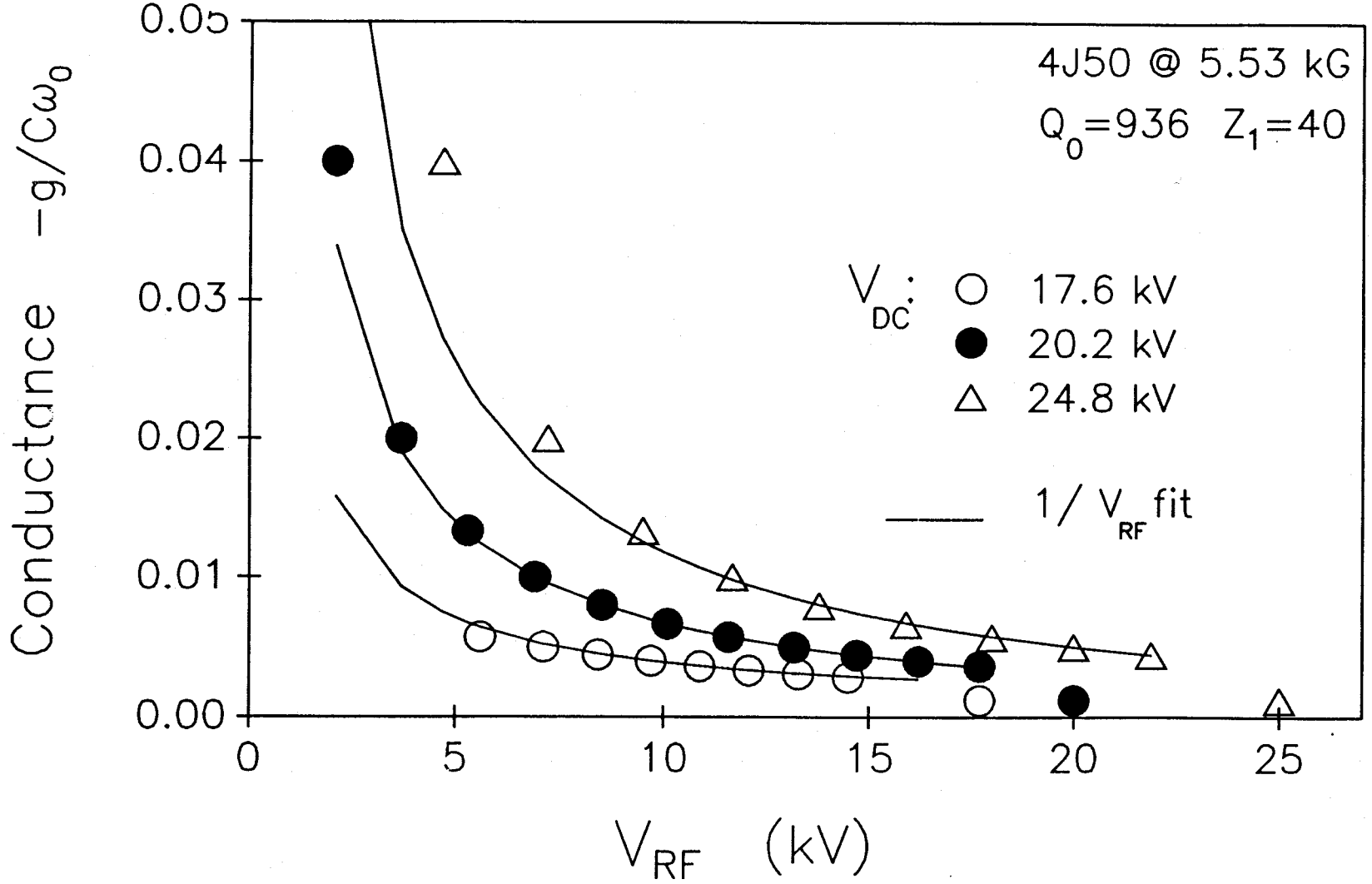

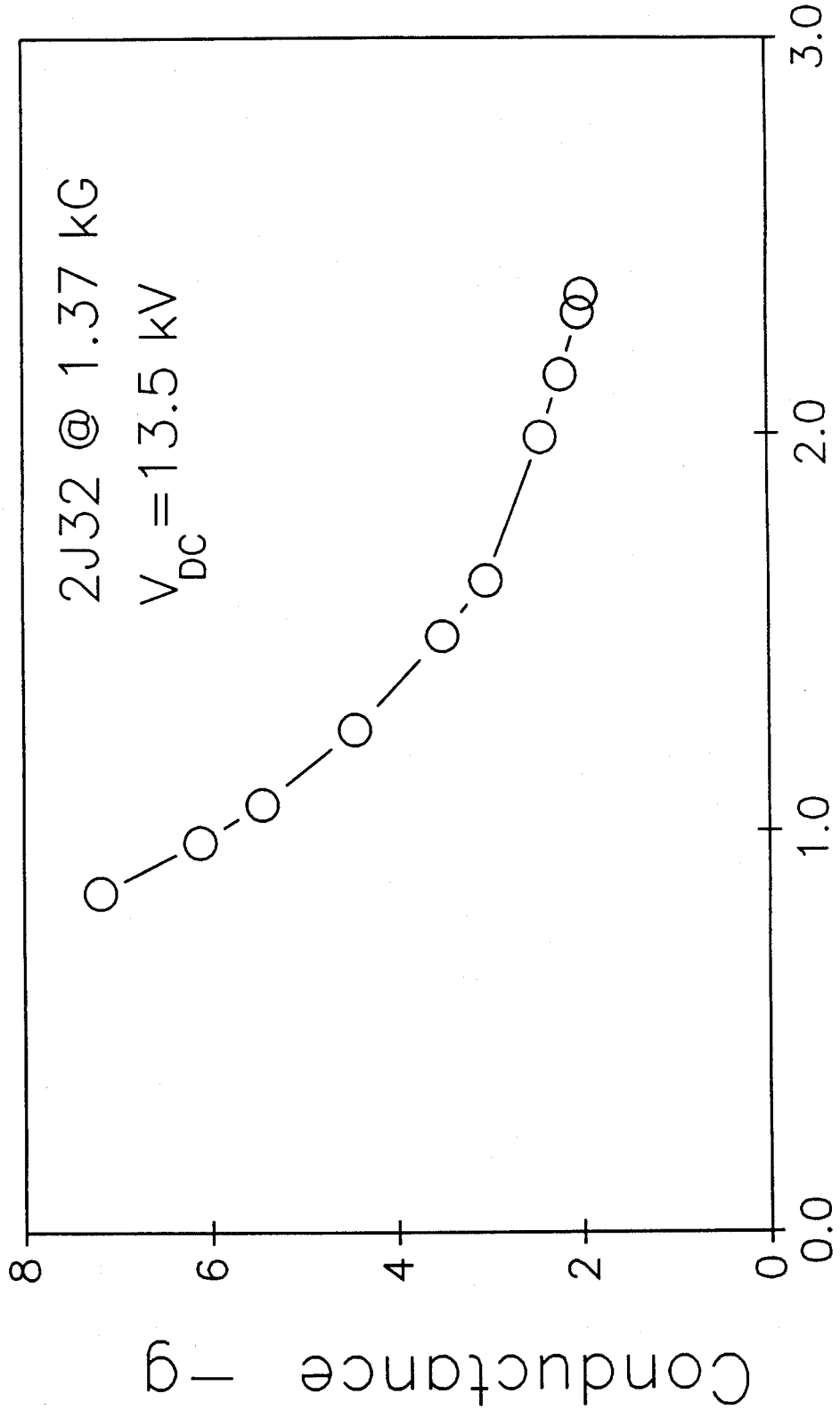

Fig. 2(b)

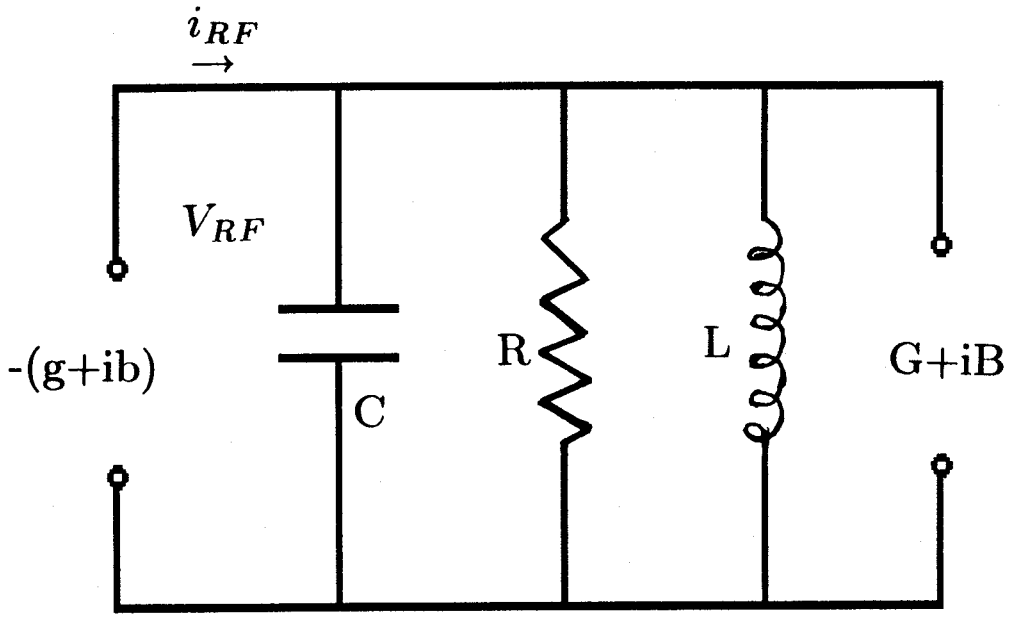

Figure 3 Equivalent circuit used in modelling magnetron operation. $g+ib$ is the complex admittance describing the electron-wave interaction. $G+iB$ represents the load admittance. RLC-circuit models the magnetron resonance cavity with loss.

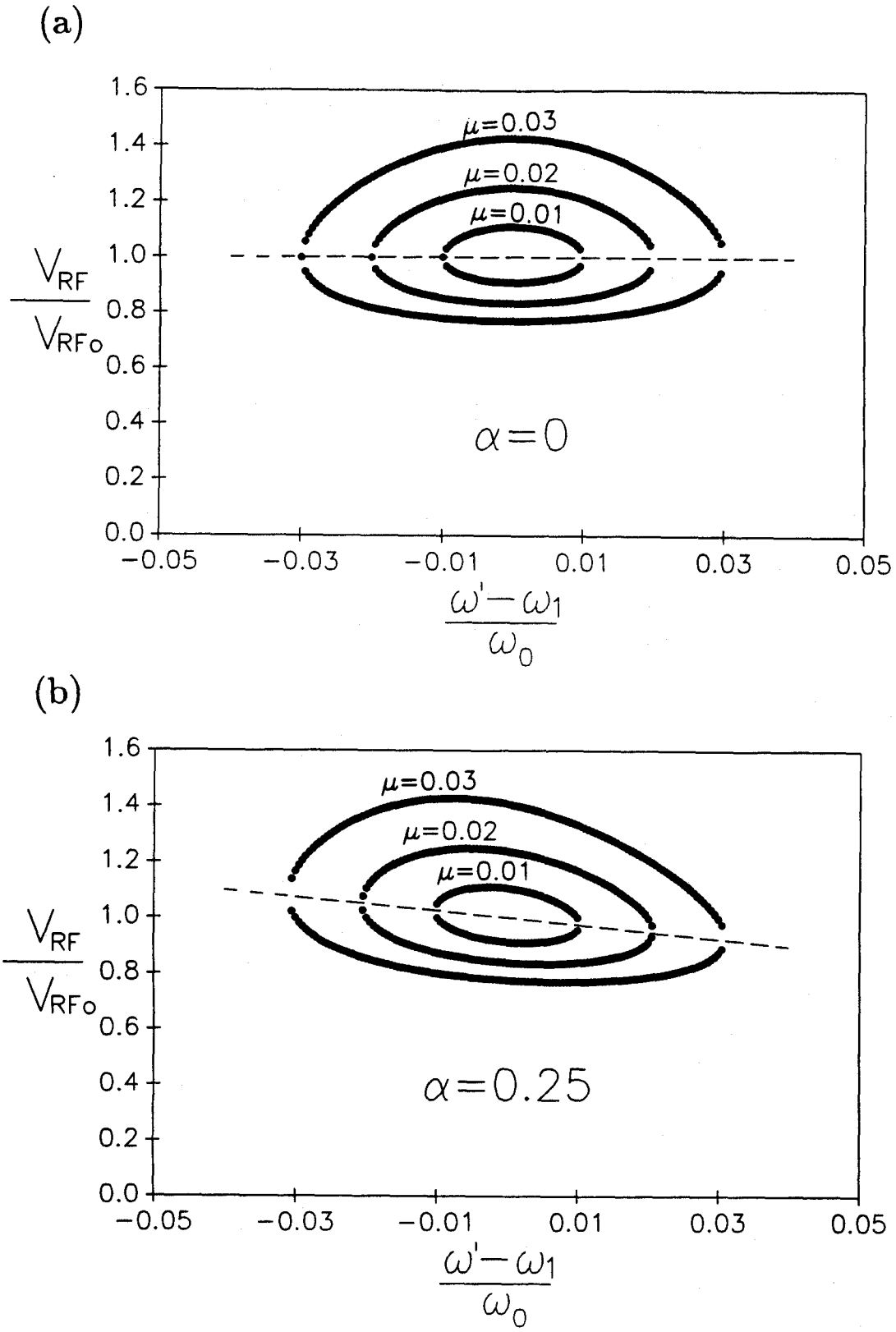

Figure 4 Amplitude ($\frac{V_{RF}}{V_{RF0}}$) versus normalized frequency difference σ in the phase-locked states for three injection amplitudes $\mu = 0.01, 0.02, 0.03$. (a) No frequency pushing, each ellipse corresponds to an injection parameter μ. (b) The effect of frequency pushing ($\alpha = 0.25$) rotates the ellipses and results in a wider locking bandwidth and a shifted amplitude resonance frequency.